

Io's active volcanoes during the New Horizons era: Insights from New Horizons imaging



J.A. Rathbun^{a,*}, J.R. Spencer^b, R.M. Lopes^c, R.R. Howell^d

^a Planetary Science Institute, 1700 E. Fort Lowell, Tucson, AZ 85719, United States

^b Southwest Research Institute, 1050 Walnut St., Suite 300, Boulder, CO 80302, United States

^c Jet Propulsion Laboratory, California Institute of Technology, 4800 Oak Grove Drive, Pasadena, CA 91109, United States

^d University of Wyoming, 1000 E. University Ave., Laramie, WY 82071, United States

ARTICLE INFO

Article history:

Received 18 April 2013

Revised 2 December 2013

Accepted 4 December 2013

Available online 12 December 2013

Keywords:

IO

Satellites, surfaces

Volcanism

ABSTRACT

In February 2007, the New Horizons spacecraft flew by the Jupiter system, obtaining images of Io, the most volcanically active body in the Solar System. The Multicolor Visible Imaging Camera (MVIC), a four-color (visible to near infrared) camera, obtained 17 sets of images. The Long-Range Reconnaissance Imager (LORRI), a high-resolution panchromatic camera, obtained 190 images, including many of Io eclipsed by Jupiter. We present a complete view of the discrete point-like emission sources in all images obtained by these two instruments. We located 54 emission sources and determined their brightnesses. These observations, the first that observed individual Ionian volcanoes on short timescales of seconds to minutes, demonstrate that the volcanoes have stable brightnesses on these timescales. The active volcanoes Tvashtar (63N, 124W) and E. Girru (22N, 245W) were observed by both LORRI and MVIC, both in the near-infrared (NIR) and methane (CH₄) filters. Tvashtar was additionally observed in the red filter, which allowed us to calculate a color temperature of approximately 1200 K. We found that, with some exceptions, most of the volcanoes frequently active during the Galileo era continued to be active during the New Horizons flyby. We found that none of the seven volcanoes observed by New Horizons multiple times over short timescales showed substantial changes on the order of seconds and only one, E. Girru exhibited substantial variation over minutes to days, increasing by 25% in just over an hour and decreasing by a factor of 4 over 6 days. Observations of Tvashtar are consistent with a current eruption similar to previously observed eruptions and are more consistent with the thermal emission of a lava flow than the fire fountains inferred from the November 1999 observations. These data also present new puzzles regarding Ionian volcanism. Since there is no associated surface change or low albedo feature that could be identified nearby, the source of the emission from E. Girru is a mystery. Furthermore, the in-eclipse glows we observe over many paterae are likely to be gas emission from interaction with the magnetosphere, but the details of that process are not clear.

© 2013 Elsevier Inc. All rights reserved.

1. Introduction

Io is the most volcanically active body in the Solar System, with more than 100 known active volcanoes emitting infrared radiation. With such a high level of activity, changes in the temperature and activity of the volcanoes are common. Observations by the Voyager, Galileo, and Cassini spacecraft and ground-based telescopes (such as NASA's Infrared Telescope Facility) have enabled determinations of changes on timescales of days to decades (Davies et al., 2001; Keszthelyi et al., 2001; Lopes et al., 2001, 2004; Rathbun et al., 2002; Radebaugh et al., 2004; Rathbun and Spencer, 2010; Davies et al., 2012). More recently, the New Horizons spacecraft

flew by the Jupiter system on its way to Pluto. Its closest approach to Io occurred on February 28th, 2007, allowing determination of changes in Ionian volcanism since the Galileo and Cassini spacecraft observations in 1995–2003 (Spencer et al., 2007). The spacecraft obtained dozens of images, many during 2 separate eclipses, potentially enabling detection of volcanic changes on timescales of seconds, minutes, and hours. For more than 3 days, the spacecraft was within 3.5 million km, close enough to obtain high quality observations covering all longitudes of Io, so a complete, unbiased view of global volcanism was obtained (with the exception that high latitudes were seen only at high emission angles, due to the equatorial nature of the flyby).

The Multicolor Visible Imaging Camera (MVIC), a four-color (visible to near infrared) camera, obtained 17 sets of images (Reuter et al., 2008). The Long-Range Reconnaissance Imager

* Corresponding author.

E-mail address: rathbun@psi.edu (J.A. Rathbun).

(LORRI), a high-resolution panchromatic camera, obtained 190 images, including 89 of Io eclipsed by Jupiter (Cheng et al., 2008). These eclipse LORRI images covered about 60% of the surface (missing longitudes 30–170W). Spencer et al. (2007) searched these data for plumes and surface changes, and found many hot spots including a previously undetected bright hotspot at 22N 245W that they designated “East Girru,” due to its location approximately 200 km east of the Girru hotspot seen by Galileo.

In this paper, we present a complete view of the discrete emission sources in all LORRI and MVIC data. We use these data to address questions regarding the state of Ionian volcanism during the 2007 flyby. 1. Which volcanoes are active? 2. Where are they located? 3. How do their locations compare to those mapped by Galileo? 4. How active are they? 5. How does the activity level compare to measurements from Galileo? 6. How does the activity vary on short time scales of seconds, minutes, and hours? In addition to addressing these questions, the New Horizons observations yielded data that present new questions that need to be addressed.

With high spatial resolution (as good as 12 km/pixel) and wide-band sensitivity covering approximately 400–900 nm (Cheng et al., 2008), LORRI is useful for detecting thermal emission from high-temperature (>1000 K) eruptions and can be used to address all of the above questions. However, it cannot differentiate between thermal and non-thermal sources. LORRI provides the most precise locations of activity because of its high angular resolution (4.95 μ rad/pixel), and can be used to study short time-scale variations due to the rapid cadence of some image sequences. With multiple bands but a lower spatial resolution and fewer observations, MVIC gives additional information on activity level and longer-term variation in the volcanoes, and can provide temperature information. Its multi-wavelength capability is also useful for distinguishing thermal and non-thermal emission.

2. Analysis

We examine all LORRI and MVIC images for bright, point-like sources on the part of Io that is not illuminated by sunlight. For each source, we determine its location and brightness. We calculate the location of each source by determining the location of Io’s limb in the image and knowing Io’s orientation at the time of the observation. For the higher resolution LORRI data we use the triaxial shape of Io for the limb fits and a spherical shape for the lower resolution MVIC images. Determining brightnesses in physical units is complicated by the necessity to assume a wavelength distribution of emission within the broad MVIC and LORRI bandpasses: we assume blackbody emission at a single fixed temperature a priori. However, reporting brightness in such units allows easier comparison to measurements from other instruments, spacecraft, and ground-based telescopes. Emission source locations and brightnesses are shown in Fig. 1. The size of each circle indicates the relative brightness of that emission source.

2.1. Calibration

Fig. 2 shows the bandpasses of the LORRI and MVIC instruments (Morgan et al., 2005). We use these to calculate the isophotal wavelength, which allows us to calculate the brightness (power per unit area per solid angle per unit wavelength) of an emitting region. The isophotal wavelength, λ_{iso} , is the wavelength at which, given a source spectrum, the monochromatic flux is the same as the mean flux through the filter, $F_{\lambda}(\lambda_{iso}) \int \lambda S(\lambda) d\lambda = \int \lambda F(\lambda) S(\lambda) d\lambda$, where F_{λ} is the brightness as a function of wavelength and $S(\lambda)$ is the spectral response (Tokunaga and Vacca, 2005). For F_{λ} we assume a blackbody at 1200 K, a typical temperature of the high temperature component of Ionian volcanoes (e.g. Milazzo et al., 2005;

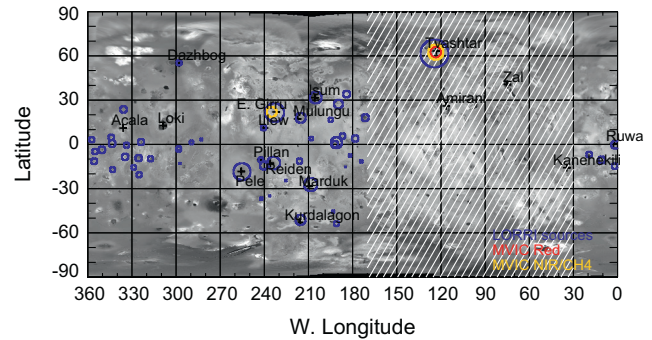


Fig. 1. Locations of all emission sources found in LORRI and MVIC images. The diameter of the circle indicates the relative brightness of that emission source with a log scale. The relative scaling of LORRI, and the two MVIC filters is arbitrary. The responses in the MVIC near infrared (NIR) and methane (CH₄) channels was nearly identical. Locations of volcanoes discussed in this paper are marked with a plus sign and label. The hatched region approximately indicates the region not covered by NH LORRI eclipse images, although shorter exposure partial daytime images did allow the detection of the very bright Tvashtar eruption.

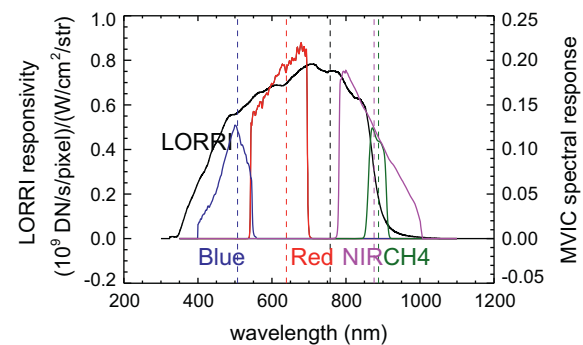


Fig. 2. Response function for LORRI and each filter in MVIC. Vertical lines indicate the effective (isophotal) wavelength for a 1200 K blackbody corresponding to each filter.

Spencer et al., 2007). From this, we calculate the isophotal wavelength for LORRI and each of the MVIC filters (Fig. 2).

For each hotspot, we calculated the total thermal emission measured by adding up the signal from pixels that include the source, and subtracting the nearby (within 6 pixels) background level, yielding a total data number and uncertainty which we converted to physical units of W/nm/str. LORRI data were converted using the responsivity in units of (DN/s/pixel)/(W/cm²/str) (Morgan et al., 2005) and multiplying by the projected area of a pixel (Table 1). MVIC data were converted using the quantum efficiency, filter transmissivity, beam splitter reflectance, and mirror reflectance to determine the percentage of incoming photons that produce an electron. We use the gain, exposure time and the isophotal wavelength to convert the measurements to physical units (Table 1).

2.2. Determining temperatures

The brightness of a volcano’s thermal emission depends on the area and temperature of exposed hot material. Temperature measurements can be used to estimate how long lava has been cooling and, in some cases, constrain the eruption temperature and, therefore, lava composition and type of eruption. Furthermore, since the determination of brightness in physical units depends on the assumed temperature, determining temperatures enables us to either confirm that we used the proper assumed temperature or

Table 1

Location and brightness of each emission source found in LORRI images. Brightness is given in physical units (assuming a 1200 K blackbody at an isophotal wavelength of 757 nm) and in DN/s. Uncertainties are included for all measurements. Images where E. Girru was used to determine location of image show 0 uncertainty for E. Girru. All angles are given in degrees (including uncertainties).

Date	Time	Lat	Unc	Lon	Unc	Power (W/nm/str)	Unc	DN/s	Unc	Emi
2/27/07	14:35:02	21.45	0	233.08	0	912.6	114.1	2000	250	76.5
2/27/07	14:35:02	-12.69	0.33	233.43	1.79	61.5	6.8	135	15	70.9
2/27/07	14:35:02	-18.61	0.46	255.49	1	615.2	68.4	1350	150	49.7
2/27/07	14:35:05	21.45	0	233.08	0	912.6	45.6	2000	100	76.5
2/27/07	14:35:05	-12.43	0.33	233.37	1.79	73.1	6.8	160	15	71
2/27/07	14:35:05	-18.59	0.46	255.55	1	639.6	45.6	1400	100	49.7
2/27/07	14:35:08	21.45	0	233.08	0	959.3	45.6	2100	100	76.5
2/27/07	14:35:08	-12.65	0.33	233.48	1.79	73.1	4.6	160	10	70.8
2/27/07	14:35:08	-18.67	0.46	255.34	1	662.0	45.6	1450	100	49.9
2/27/07	14:45:02	21.45	0	233.08	0	913.8	45.7	2000	100	77.5
2/27/07	14:45:02	-12.62	0.33	233.74	1.8	73.2	3.4	160	7.5	71.6
2/27/07	14:45:02	-18.67	0.46	255.19	1	685.4	45.7	1500	100	51
2/27/07	14:45:05	21.45	0	233.08	0	707.8	68.5	1550	150	77.5
2/27/07	14:45:05	-12.59	0.33	233.59	1.81	52.6	9.1	115	20	71.8
2/27/07	14:45:05	-18.55	0.46	255.57	0.99	526.2	68.5	1150	150	50.7
2/27/07	14:45:08	21.45	0	233.08	0	936.3	45.7	2050	100	77.5
2/27/07	14:45:08	-12.59	0.33	233.58	1.81	75.5	4.6	165	10	71.8
2/27/07	14:45:08	-18.53	0.46	255.48	0.99	685.4	22.8	1500	50	50.8
2/27/07	14:55:02	21.45	0	233.08	0	778.2	68.6	1700	150	78.4
2/27/07	14:55:02	-12.6	0.33	233.68	1.84	64.1	6.9	140	15	72.7
2/27/07	14:55:02	-18.54	0.46	255.4	0.99	594.4	68.6	1300	150	51.8
2/27/07	14:55:05	-12.4	0.31	232.71	1.93	45.8	18.3	100	40	73.7
2/27/07	14:55:05	21.45	0	233.08	0	435.0	68.6	950	150	78.4
2/27/07	14:55:05	-18.78	0.46	255.63	0.98	365.6	91.5	800	200	51.6
2/27/07	14:55:08	-0.29	0.85	1.66	1.68	21.2	2.1	46.5	4.5	53.5
2/27/07	14:55:08	-14.85	0.83	1.94	1.45	9.6	1.1	21	2.5	52.1
2/27/07	14:55:08	-10.56	0.89	10.68	1.9	16.0	6.9	35	15	44.2
2/27/07	14:55:08	-6.89	1.02	19.24	2.84	9.8	3.0	21.5	6.5	38.6
2/27/07	14:55:08	21.44	0.26	232.3	3.77	502.5	91.5	1100	200	22.9
2/27/07	14:55:08	-12.67	0.18	232.69	4.01	43.5	6.9	95	15	12.2
2/27/07	14:55:08	21.45	0	233.08	0	847.6	45.8	1850	100	78.5
2/27/07	14:55:08	-12.68	0.33	234.03	1.81	54.9	9.2	120	20	72.4
2/27/07	14:55:08	-18.59	0.46	255.72	0.98	641.3	22.9	1400	50	51.5
2/27/07	14:55:08	-18.83	0.51	256.03	1.9	457.5	68.6	1000	150	24
2/27/07	14:55:08	55.28	1.42	297.99	1.42	8.2	0.7	18	1.5	24.5
2/27/07	14:55:08	-2.55	0.65	298.1	1.01	5.5	0.9	12	2	59.2
2/27/07	14:55:08	-9.81	0.69	317.37	1	8.2	2.1	18	4.5	60.9
2/27/07	14:55:08	1.53	0.71	323.81	1.03	11.4	1.8	25	4	64.9
2/27/07	14:55:08	-20.67	0.73	325.14	1.02	8.7	0.9	19	2	69.4
2/27/07	14:55:08	-9.32	0.71	325.52	1.01	13.1	2.3	28.5	5	52.6
2/27/07	14:55:08	-15.65	0.72	328.81	1.02	6.6	1.1	14.5	2.5	34.9
2/27/07	14:55:08	-0.56	0.73	333.75	1.1	8.0	1.1	17.5	2.5	54.2
2/27/07	14:55:08	-8.51	0.73	334.65	1.06	14.2	2.3	31	5	47
2/27/07	14:55:08	23.71	0.86	335.76	1.43	14.6	1.8	32	4	9
2/27/07	14:55:08	-17.16	0.76	343.11	1.1	7.8	1.4	17	3	46.3
2/27/07	14:55:08	0.56	0.76	343.49	1.22	15.3	3.2	33.5	7	31.3
2/27/07	14:55:08	4.74	0.78	344.1	1.28	9.8	1.4	21.5	3	59
2/27/07	14:55:08	-3.7	0.78	350.44	1.3	15.6	1.6	34	3.5	28.6
2/27/07	14:55:08	-4.89	0.8	355.11	1.39	9.2	0.9	20	2	28.3
2/27/07	14:55:08	-11.48	0.8	355.7	1.33	11.0	1.1	24	2.5	62.8
2/27/07	14:55:08	3.14	0.83	357.29	1.59	8.5	0.9	18.5	2	33
2/27/07	14:55:08	-55	3	292	9	5.494	0.686	12	2	100
2/27/07	15:13:01	21.45	0	233.08	0	808.1	64.3	1760	140	80.1
2/27/07	15:13:01	-12.8	0.33	234.59	1.83	64.3	9.2	140	20	73.7
2/27/07	15:13:01	-18.57	0.46	255.56	0.97	586.4	36.6	1280	80	53.5
2/27/07	15:13:02	21.45	0	233.08	0	742.4	18.3	1620	40	80.1
2/27/07	15:13:02	-12.64	0.32	234.1	1.87	100.9	55.1	220	120	74.2
2/27/07	15:13:02	-18.53	0.46	255.49	0.97	578.9	18.3	1260	40	53.5
2/27/07	15:13:03	21.45	0	233.08	0	742.4	18.3	1620	40	80.1
2/27/07	15:13:03	-12.68	0.32	234.13	1.87	110.1	64.3	240	140	74.1
2/27/07	15:13:03	-18.59	0.46	255.56	0.97	586.4	18.3	1280	40	53.5
2/27/07	15:15:02	21.45	0	233.08	0	665.5	68.8	1450	150	80.3
2/27/07	15:15:02	-12.52	0.32	234.14	1.87	61.8	20.7	135	45	74.3
2/27/07	15:15:02	-18.6	0.46	255.76	0.96	573.4	45.9	1250	100	53.5
2/27/07	15:15:05	-12.49	0.31	233.04	1.99	64.3	11.5	140	25	75.4
2/27/07	15:15:05	21.45	0	233.08	0	735.0	22.9	1600	50	80.3
2/27/07	15:15:05	-18.61	0.46	255.5	0.97	550.8	45.9	1200	100	53.8
2/27/07	15:15:08	21.45	0	233.08	0	413.6	137.6	900	300	80.3
2/27/07	15:15:08	-14.37	0.38	240.35	1.44	22.9	9.2	50	20	68.2
2/27/07	15:15:08	-18.62	0.46	255.79	0.96	321.5	91.7	700	200	53.5
2/27/07	15:26:02	-12.28	0.29	232.65	2.1	39.0	13.8	85	30	76.9
2/27/07	15:26:02	21.45	0	233.09	0	436.7	137.8	950	300	81.4

(continued on next page)

Table 1 (continued)

Date	Time	Lat	Unc	Lon	Unc	Power (W/nm/str)	Unc	DN/s	Unc	Emi
2/27/07	15:26:02	-18.85	0.47	256.14	0.95	414.1	114.8	900	250	54.3
2/27/07	15:26:05	21.45	0	233.09	0	688.9	45.9	1500	100	81.4
2/27/07	15:26:05	-12.65	0.31	233.74	1.97	64.4	9.2	140	20	75.8
2/27/07	15:26:05	-18.57	0.46	255.59	0.96	574.1	45.9	1250	100	54.8
2/27/07	15:26:08	21.45	0	233.09	0	689.0	29.9	1500	65	81.4
2/27/07	15:26:08	-12.62	0.31	233.55	1.99	61.9	6.9	135	15	76
2/27/07	15:26:08	-18.55	0.46	255.53	0.96	574.1	23.0	1250	50	54.8
2/27/07	15:45:01	21.45	0	233.09	0	581.0	64.5	1260	140	83.2
2/27/07	15:45:01	-12.67	0.32	234.83	1.94	73.8	27.5	160	60	76.7
2/27/07	15:45:01	-18.63	0.47	255.83	0.94	533.9	92.1	1160	200	56.4
2/27/07	15:45:02	21.45	0	233.09	0	607.4	46.0	1320	100	83.2
2/27/07	15:45:02	-12.61	0.29	233.41	2.13	92.1	18.4	200	40	78.1
2/27/07	15:45:02	-18.61	0.47	255.73	0.94	515.0	36.8	1120	80	56.5
2/27/07	15:45:03	21.53	0	232.43	0	562.2	46.0	1220	100	83.8
2/27/07	15:45:03	-12.69	0.3	233.7	2.09	46.0	18.4	100	40	77.8
2/27/07	15:45:03	-18.58	0.47	255.48	0.94	533.9	18.4	1160	40	56.7
2/27/07	15:48:02	21.45	0	233.09	0	598.2	46.0	1300	100	83.4
2/27/07	15:48:02	-12.52	0.28	233.11	2.19	50.6	9.2	110	20	78.7
2/27/07	15:48:02	-18.63	0.47	255.73	0.94	530.3	23.0	1150	50	56.8
2/27/07	15:48:05	21.45	0	233.09	0	530.3	23.0	1150	50	83.4
2/27/07	15:48:05	-12.59	0.29	233.34	2.16	39.1	9.2	85	20	78.5
2/27/07	15:48:05	-18.6	0.47	255.71	0.94	530.3	46.0	1150	100	56.8
3/1/07	0:35:16	62.15	0.29	123.24	0.59	52230.9	4606.4	170,000	15,000	73.1
3/1/07	0:35:19	62.14	0.29	123.03	0.59	47574.9	2303.2	155,000	7500	73.2
3/1/07	0:35:22	61.56	0.29	124.21	0.59	45058.4	4090.5	146,667	13,333	72.4
3/1/07	2:28:31	61.25	0.41	126.03	1.02	30761.7	2640.5	95,455	8181.8	76.9
3/1/07	2:28:51	61.57	0.28	124.89	0.69	30635.2	3222.0	95,000	10,000	77.5
3/1/07	2:28:54	61.93	0.28	124.6	0.69	30107.8	2152.4	93,333	6666.7	77.9
3/1/07	7:36:19	21.38	0.44	233.22	1.23	1794.0	309.7	4350	750	25.9
3/1/07	7:36:22	21.53	0.44	232.96	1.23	1743.4	137.8	4200	333.3	26
3/1/07	9:30:01	21.45	0	233.07	0	2329.9	233.0	5000	500	24
3/1/07	9:30:01	-12.65	0.48	233.5	1.15	177.0	46.6	380	100	11.3
3/1/07	9:30:01	-18.52	0.47	255	1.29	1164.9	139.8	2500	300	23.7
3/1/07	9:30:02	21.45	0	233.07	0	1909.8	233.0	4100	500	24
3/1/07	9:30:02	-12.65	0.48	233.37	1.15	255.9	46.6	550	100	11.3
3/1/07	9:30:02	-18.49	0.47	254.93	1.29	979.7	93.2	2100	200	23.6
3/1/07	9:30:03	21.45	0	233.07	0	2100.8	233.0	4500	500	24
3/1/07	9:30:03	-12.6	0.48	233.57	1.15	210.1	46.6	450	100	11.2
3/1/07	9:30:03	-18.51	0.47	254.9	1.29	1025.6	139.8	2200	300	23.6
3/1/07	9:30:04	21.45	0	233.07	0	2100.8	233.0	4500	500	24
3/1/07	9:30:04	-12.74	0.48	233.72	1.15	233.0	93.2	500	200	11.3
3/1/07	9:30:04	-18.62	0.47	254.97	1.3	1025.6	139.8	2200	300	23.7
3/1/07	9:30:05	21.45	0	233.07	0	2100.9	233.0	4500	500	24
3/1/07	9:30:05	-12.65	0.48	233.54	1.15	278.8	93.2	600	200	11.3
3/1/07	9:30:05	-18.69	0.47	254.98	1.3	1071.4	139.8	2300	300	23.8
3/1/07	9:30:06	21.45	0	233.07	0	2139.1	233.0	4600	500	24
3/1/07	9:30:06	-12.62	0.48	233.66	1.15	163.1	46.6	350	100	11.2
3/1/07	9:30:06	-18.65	0.47	254.94	1.3	932.0	93.2	2000	200	23.7
3/1/07	9:30:07	21.45	0	233.07	0	2005.4	186.4	4300	400	24
3/1/07	9:30:07	-12.76	0.48	233.65	1.15	210.1	69.9	450	150	11.3
3/1/07	9:30:07	-18.56	0.47	254.96	1.29	1025.6	139.8	2200	300	23.7
3/1/07	9:30:08	21.45	0	233.07	0	2101.0	233.0	4500	500	24
3/1/07	9:30:08	-12.77	0.48	233.66	1.15	210.1	46.6	450	100	11.3
3/1/07	9:30:08	-18.5	0.47	254.57	1.29	1025.7	93.2	2200	200	23.4
3/1/07	9:30:09	21.45	0	233.07	0	2139.2	139.8	4600	300	24
3/1/07	9:30:09	-12.72	0.48	233.68	1.15	139.8	46.6	300	100	11.3
3/1/07	9:30:09	-18.53	0.47	255.16	1.3	979.8	93.2	2100	200	23.8
3/1/07	9:30:10	21.45	0	233.07	0	2101.0	139.8	4500	300	24
3/1/07	9:30:10	-12.81	0.48	233.34	1.15	233.0	46.6	500	100	11.5
3/1/07	9:30:10	-18.51	0.47	254.65	1.29	1071.5	139.8	2300	300	23.4
3/1/07	9:30:11	21.45	0	233.07	0	2139.3	466.1	4600	1000	24
3/1/07	9:30:11	-12.71	0.48	233.4	1.15	278.9	69.9	600	150	11.4
3/1/07	9:30:11	-18.56	0.47	254.96	1.29	979.9	139.8	2100	300	23.7
3/1/07	9:30:12	21.45	0	233.07	0	2101.1	233.0	4500	500	24
3/1/07	9:30:12	-12.62	0.48	233.69	1.15	233.0	46.6	500	100	11.2
3/1/07	9:30:12	-18.53	0.47	254.92	1.29	979.9	93.2	2100	200	23.6
3/1/07	9:30:13	21.45	0	233.07	0	2330.4	466.1	5000	1000	24
3/1/07	9:30:13	-12.9	0.48	233.36	1.15	139.8	46.6	300	100	11.6
3/1/07	9:30:13	-18.55	0.47	254.9	1.29	1025.7	93.2	2200	200	23.6
3/1/07	9:30:14	21.45	0	233.07	0	2330.4	233.0	5000	500	24
3/1/07	9:30:14	-12.56	0.48	233.57	1.15	186.4	46.6	400	100	11.2
3/1/07	9:30:14	-18.76	0.47	255	1.3	1025.8	93.2	2200	200	23.8
3/1/07	9:30:15	21.45	0	233.07	0	2330.5	139.8	5000	300	24
3/1/07	9:30:15	-12.63	0.48	233.59	1.15	233.0	46.6	500	100	11.2
3/1/07	9:30:15	-18.65	0.47	254.78	1.29	1071.6	93.2	2300	200	23.6

Table 1 (continued)

Date	Time	Lat	Unc	Lon	Unc	Power (W/nm/str)	Unc	DN/s	Unc	Emi
3/1/07	9:30:16	21.45	0	233.07	0	2292.3	186.4	4900	400	24
3/1/07	9:30:16	-12.8	0.48	233.55	1.15	93.2	46.6	200	100	11.4
3/1/07	9:30:16	-18.65	0.47	254.92	1.29	980.0	93.2	2100	200	23.7
3/1/07	9:30:17	21.45	0	233.07	0	2101.3	186.4	4500	400	24
3/1/07	9:30:17	-12.69	0.48	233.51	1.15	278.9	46.6	600	100	11.3
3/1/07	9:30:17	-18.57	0.47	254.92	1.29	1025.8	93.2	2200	200	23.6
3/1/07	9:30:18	21.45	0	233.07	0	1967.6	186.4	4200	400	24
3/1/07	9:30:18	-12.71	0.48	233.65	1.15	139.8	46.6	300	100	11.3
3/1/07	9:30:18	-18.36	0.47	254.84	1.29	1119.4	93.2	2400	200	23.4
3/1/07	9:30:19	21.45	0	233.07	0	2101.4	233.1	4500	500	24
3/1/07	9:30:19	-12.42	0.48	233.47	1.15	233.1	46.6	500	100	11.1
3/1/07	9:30:19	-18.37	0.47	254.71	1.29	1025.9	139.8	2200	300	23.4
3/1/07	9:30:20	21.45	0	233.07	0	2139.6	139.8	4600	300	24
3/1/07	9:30:20	-18.39	0.47	254.91	1.29	1025.9	93.2	2200	200	23.5
3/1/07	9:30:21	21.45	0	233.07	0	2197.0	186.5	4700	400	24
3/1/07	9:30:21	-12.48	0.48	233.48	1.15	116.5	46.6	250	100	11.1
3/1/07	9:30:21	-18.52	0.47	254.89	1.29	1025.9	93.2	2200	200	23.6
3/1/07	9:30:22	21.45	0	233.07	0	2139.7	139.8	4600	300	24
3/1/07	9:30:22	-12.59	0.48	233.48	1.15	139.8	46.6	300	100	11.2
3/1/07	9:30:22	-18.43	0.47	254.9	1.29	980.1	93.2	2100	200	23.5
3/1/07	9:30:23	21.45	0	233.07	0	2101.5	186.5	4500	400	24
3/1/07	9:30:23	-12.25	0.48	233.45	1.15	278.9	93.2	600	200	10.9
3/1/07	9:30:23	-18.4	0.47	254.9	1.29	980.1	93.2	2100	200	23.5
3/1/07	9:30:24	21.45	0	233.07	0	2139.8	139.9	4600	300	24
3/1/07	9:30:24	-12.75	0.48	233.63	1.15	233.1	69.9	500	150	11.3
3/1/07	9:30:24	-18.46	0.47	254.99	1.29	1119.6	93.2	2400	200	23.6
3/1/07	9:30:25	21.45	0	233.07	0	2139.8	186.5	4600	400	24
3/1/07	9:30:25	-12.6	0.48	233.57	1.15	186.5	46.6	400	100	11.2
3/1/07	9:30:25	-18.48	0.47	254.91	1.29	980.1	93.2	2100	200	23.6
3/1/07	9:30:26	21.45	0	233.07	0	2139.9	186.5	4600	400	24
3/1/07	9:30:26	-12.56	0.48	233.61	1.15	233.1	93.2	500	200	11.2
3/1/07	9:30:26	-18.43	0.47	254.82	1.29	1026.0	139.9	2200	300	23.5
3/1/07	9:30:27	21.45	0	233.07	0	2331.0	186.5	5000	400	24
3/1/07	9:30:27	-12.42	0.48	233.61	1.15	233.1	46.6	500	100	11
3/1/07	9:30:27	-18.47	0.47	254.93	1.29	1026.0	139.9	2200	300	23.6
3/1/07	9:30:28	21.45	0	233.07	0	2139.9	186.5	4600	400	24
3/1/07	9:30:28	-12.64	0.48	233.59	1.15	186.5	46.6	400	100	11.2
3/1/07	9:30:28	-18.44	0.47	255.18	1.3	1119.7	139.9	2400	300	23.7
3/1/07	9:30:29	21.45	0	233.07	0	2101.8	186.5	4500	400	24
3/1/07	9:30:29	-12.47	0.48	233.48	1.15	279.0	69.9	600	150	11.1
3/1/07	9:30:29	-18.5	0.47	255.06	1.29	932.4	139.9	2000	300	23.7
3/1/07	9:30:30	21.45	0	233.07	0	2235.6	233.1	4800	500	24
3/1/07	9:30:30	-12.68	0.48	233.5	1.15	139.9	46.6	300	100	11.3
3/1/07	9:30:30	-18.54	0.47	254.88	1.29	932.4	139.9	2000	300	23.6
3/1/07	9:35:04	27.32	2.44	188.7	10.54	35.3	5.9	75.3	12.6	70.7
3/1/07	9:35:04	31.1	2.41	203.54	8.37	117.7	29.4	251	62.8	84.1
3/1/07	9:35:04	-52.32	3.1	213.76	7.48	64.7	17.6	138.1	37.7	89.5
3/1/07	9:35:04	19.36	2.1	214.49	6.3	53.0	17.6	113	37.7	93.3
3/1/07	9:35:12	27.76	2.46	188.57	10.65	29.4	5.9	62.8	12.6	70.7
3/1/07	9:35:12	31.46	2.41	204.97	8.24	117.7	29.4	251	62.8	85.3
3/1/07	9:35:12	-50.59	3	213.95	7.3	58.8	17.7	125.5	37.7	89.8
3/1/07	9:35:12	18.2	2.09	214.58	6.23	70.7	17.7	150.6	37.7	93.3
3/1/07	9:35:20	33.45	2.48	204.43	8.58	111.8	11.8	238.5	25.1	85.1
3/1/07	9:35:20	21.48	2.13	215.44	6.38	47.1	17.7	100.4	37.7	94.2
3/1/07	9:35:20	-48.1	2.85	216.21	7.08	53.0	17.7	113	37.7	91.4
3/1/07	9:35:28	26.5	2.4	191.21	9.83	39.4	5.3	84.1	11.3	72.7
3/1/07	9:35:28	29.82	2.36	205.39	7.98	105.9	5.9	225.9	12.6	85.6
3/1/07	9:35:28	19.12	2.1	215.28	6.25	53.0	17.7	113	37.7	94
3/1/07	9:35:28	-51.53	3.04	216.19	7.44	58.8	17.7	125.5	37.7	91.1
3/1/07	9:35:36	27.66	2.44	190.35	10.21	34.8	5.3	74.1	11.3	72.2
3/1/07	9:35:36	31.82	2.42	205.96	8.17	123.6	11.8	263.6	25.1	86.2
3/1/07	9:35:36	-50.16	2.96	216.58	7.29	47.1	17.7	100.4	37.7	91.5
3/1/07	9:35:44	27.17	2.44	188.9	10.49	17.7	5.9	37.7	12.6	70.9
3/1/07	9:35:44	30.49	2.38	205.31	8.08	135.5	17.7	288.7	37.7	85.6
3/1/07	9:35:44	-50.6	3	214.49	7.31	53.0	11.8	113	25.1	90.1
3/1/07	9:35:44	17	2.07	214.99	6.15	58.8	17.7	125.5	37.7	93.8
3/1/07	9:35:52	27.64	2.45	189.45	10.43	35.4	11.8	75.3	25.1	71.5
3/1/07	9:35:52	31.33	2.41	204.94	8.24	111.9	11.8	238.5	25.1	85.4
3/1/07	9:35:52	-51.8	3.07	214.04	7.43	53.0	23.6	113	50.2	89.8
3/1/07	9:35:52	17.57	2.08	214.88	6.19	47.1	17.7	100.4	37.7	93.7
3/1/07	9:36:49	26.57	2.42	189.5	10.28	35.4	11.8	75.3	25.1	71.4
3/1/07	9:36:49	31.45	2.41	205.13	8.25	123.7	23.7	263.6	50.2	85.6
3/1/07	9:36:49	-27.62	2.21	207.38	6.1	153.2	11.8	326.3	25.1	85.3
3/1/07	9:36:49	-51.21	3.03	214.39	7.38	58.9	17.7	125.5	37.7	90.1
3/1/07	9:36:57	27.69	2.46	188.18	10.82	43.7	5.9	92.9	12.6	70.5

(continued on next page)

Table 1 (continued)

Date	Time	Lat	Unc	Lon	Unc	Power (W/nm/str)	Unc	DN/s	Unc	Emi
3/1/07	9:36:57	1.12	2.08	191.1	7.68	76.6	23.7	163.2	50.2	69.6
3/1/07	9:36:57	31.07	2.4	204.88	8.23	100.3	29.4	213.4	62.8	85.4
3/1/07	9:36:57	-27.24	2.21	207.77	6.08	165.1	17.7	351.4	37.7	85.7
3/1/07	9:36:57	-51.3	3.04	213.08	7.38	58.9	17.7	125.5	37.7	89.3
3/1/07	9:36:57	17.63	2.08	214.57	6.22	76.6	23.7	163.2	50.2	93.5
3/1/07	9:37:05	28.92	2.48	189.5	10.69	17.7	11.8	37.7	25.1	71.9
3/1/07	9:37:05	32.05	2.43	204.62	8.4	94.3	29.4	200.8	62.8	85.3
3/1/07	9:37:05	-25.82	2.18	208.92	6	165.1	5.9	351.4	12.6	86.7
3/1/07	9:37:05	19.92	2.11	215.37	6.31	58.9	17.7	125.5	37.7	94.3
3/1/07	9:37:05	-49.52	2.92	216.78	7.24	64.9	17.7	138.1	37.7	91.8
3/1/07	9:37:13	26.61	2.42	189.47	10.31	41.2	11.8	87.9	25.1	71.4
3/1/07	9:37:13	30.62	2.39	205.09	8.15	118.0	29.5	251	62.8	85.6
3/1/07	9:37:13	-27.79	2.22	207.01	6.13	165.2	11.8	351.4	25.1	85.1
3/1/07	9:37:13	-50.67	3	214.67	7.33	41.2	23.7	87.9	50.2	90.4
3/1/07	9:37:13	17.85	2.08	214.71	6.23	64.9	17.7	138.1	37.7	93.7
3/1/07	9:37:21	27.15	2.44	188.4	10.68	41.2	5.9	87.9	12.6	70.6
3/1/07	9:37:21	31.8	2.42	204.57	8.38	100.3	41.2	213.4	87.9	85.2
3/1/07	9:37:21	-26.43	2.19	207.36	6.08	165.2	23.7	351.4	50.2	85.4
3/1/07	9:37:21	-50.48	2.99	214.35	7.31	58.9	23.7	125.5	50.2	90.2
3/1/07	9:37:21	18.61	2.09	214.44	6.29	70.8	17.7	150.6	37.7	93.5
3/1/07	9:37:29	27.71	2.48	186.88	11.21	29.5	11.8	62.8	25.1	69.5
3/1/07	9:37:29	31.25	2.4	205.05	8.24	106.1	35.4	225.9	75.3	85.6
3/1/07	9:37:29	-25.49	2.17	208.49	6.01	171.0	11.8	364	25.1	86.4
3/1/07	9:37:29	-49.72	2.94	215.77	7.25	53.1	23.7	113	50.2	91.2
3/1/07	9:37:37	27.78	2.41	192.9	9.73	17.7	5.9	37.7	12.6	74.7
3/1/07	9:37:37	32.14	2.41	207.86	8.03	70.9	35.4	150.6	75.3	88.1
3/1/07	9:37:37	-25.89	2.17	210.83	5.93	147.5	53.2	313.8	113	88.5
3/1/07	9:37:37	17.77	2.07	217.38	6.08	47.2	29.5	100.4	62.8	96.3
3/1/07	9:37:37	-50.66	2.98	218.85	7.4	53.2	23.7	113	50.2	93.1
3/1/07	9:38:42	-30.12	2.27	206.34	6.24	188.9	23.7	401.7	50.2	84.7
3/1/07	9:38:42	-54.18	3.24	212.09	7.67	59.0	29.5	125.5	62.8	88.8
3/1/07	9:38:50	-31.71	2.31	205.77	6.32	177.2	29.5	376.6	62.8	84.2
3/1/07	9:38:50	-56.56	3.44	211.13	7.92	71.0	29.5	150.6	62.8	88.2
3/1/07	9:39:06	-57.29	3.47	217.07	8.22	47.3	29.5	100.4	62.8	91.4
3/1/07	9:39:06	-16.91	1.96	236.76	5.4	177.3	41.3	376.6	87.9	113.6
3/1/07	9:39:14	-27.02	2.19	212.44	5.92	189.1	29.5	401.7	62.8	90.1
3/1/07	9:39:14	-51.14	3	221.18	7.51	71.0	35.5	150.6	75.3	94.6
3/1/07	9:39:22	-26.34	2.2	207.23	6.1	189.1	29.5	401.7	62.8	85.5
3/1/07	9:39:22	-51.2	3.03	215.31	7.4	76.8	23.7	163.2	50.2	90.9
3/1/07	9:40:19	-26.07	2.19	209.45	6.01	171.5	29.6	364	62.8	87.6
3/1/07	9:40:19	-49.38	2.92	217.68	7.24	71.1	29.6	150.6	62.8	92.7
3/1/07	9:40:19	-11.89	1.93	234.47	5.28	224.0	17.8	477	37.7	112.4
3/1/07	9:40:27	-25.31	2.17	209.65	5.98	195.1	17.8	414.2	37.7	87.8
3/1/07	9:40:27	18.48	2.09	215.52	6.25	59.1	17.8	125.5	37.7	94.9
3/1/07	9:40:27	-11.58	1.93	233.93	5.28	212.5	11.8	451.9	25.1	111.9
3/1/07	9:40:35	-29.48	2.25	209.74	6.1	183.5	17.8	389.1	37.7	87.8
3/1/07	9:40:35	-53.82	3.2	217.85	7.76	53.3	29.6	113	62.8	92.3
3/1/07	9:40:35	-14.03	1.94	235.32	5.33	218.3	11.8	464.4	25.1	112.9
3/1/07	9:40:43	18.06	0.69	171.44	5.95	16.3	7.4	138.1	62.8	69.4
3/1/07	9:40:43	-11.6	0.66	174.11	5.96	3.0	3.0	25.1	25.1	65
3/1/07	9:40:43	3.97	0.69	178.32	4.7	13.3	5.9	113	50.2	60.9
3/1/07	9:40:43	-7.6	0.71	181.77	4.5	3.0	3.0	25.1	25.1	57.2
3/1/07	9:40:43	34.04	0.92	184.14	4.01	14.8	4.4	125.5	37.7	62.8
3/1/07	9:40:43	-15.29	0.74	184.94	4.4	1.5	1.5	12.6	12.6	54.8
3/1/07	9:40:43	5.58	0.74	186.89	3.72	9.6	4.4	81.6	37.7	52.6
3/1/07	9:40:43	-53.87	1.19	191.04	7.78	7.4	1.9	62.8	16.3	64.9
3/1/07	9:40:43	26.31	0.87	191.94	3.35	40.0	5.9	338.9	50.2	53.5
3/1/07	9:40:43	0.18	0.75	192.03	3.41	11.8	7.4	100.4	62.8	47
3/1/07	9:40:43	-45.59	1.03	193.27	5.88	2.8	1.9	23.8	16.3	59
3/1/07	9:40:43	16.7	0.81	194.95	3.14	5.9	3.0	50.2	25.1	47.3
3/1/07	9:40:43	37.86	1.04	202.79	3.07	10.3	4.4	87.9	37.7	52.1
3/1/07	9:40:43	30.09	0.95	207.28	2.83	125.6	22.2	1066.9	188.3	44.2
3/1/07	9:40:43	3.92	0.8	208.18	2.68	4.4	3.0	37.7	25.1	31.3
3/1/07	9:40:43	-28.21	0.88	209.21	3.32	162.8	29.6	1380.7	251	38.6
3/1/07	9:40:43	-26.88	2.2	210.62	5.99	189.4	23.8	401.7	50.2	88.7
3/1/07	9:40:43	-41.31	1.03	211.68	3.97	1.9	0.7	16.3	6.3	46.3
3/1/07	9:40:43	13.65	0.84	214.87	2.54	1.0	0.9	8.8	7.5	28.6
3/1/07	9:40:43	-11.36	0.82	216.13	2.65	8.9	4.4	75.3	37.7	24.5
3/1/07	9:40:43	-51.79	3.07	216.34	7.48	59.1	23.8	125.5	50.2	91.6
3/1/07	9:40:43	-52.95	1.28	216.39	4.92	19.2	7.4	163.2	62.8	54.2
3/1/07	9:40:43	16.36	0.86	217.19	2.52	26.6	7.4	225.9	62.8	28.3
3/1/07	9:40:43	-24.53	0.89	225.53	2.74	2.1	1.5	17.6	12.6	25.9
3/1/07	9:40:43	27.1	0.96	231.08	2.58	4.4	3.7	37.7	31.4	30.2
3/1/07	9:40:43	20.4	0.91	234.55	2.48	516.9	103.4	4393.1	878.6	22.9
3/1/07	9:40:43	-13.53	0.85	234.57	2.43	222.2	14.8	1882.8	125.5	12.2

Table 1 (continued)

Date	Time	Lat	Unc	Lon	Unc	Power (W/nm/str)	Unc	DN/s	Unc	Emi
3/1/07	9:40:43	−34.96	1	236.36	2.89	1.6	1.0	13.8	8.8	33
3/1/07	9:40:43	11.29	0.87	240.58	2.39	8.9	2.2	75.3	18.8	13.5
3/1/07	9:40:43	−36.84	1.03	242.15	2.89	3.0	1.9	25.1	16.3	34.9
3/1/07	9:40:43	−10.46	0.86	242.42	2.38	7.4	3.0	62.8	25.1	9
3/1/07	9:40:43	−19.36	0.91	255.95	2.5	531.4	59.4	4518.6	502.1	24
3/1/07	9:40:43	−24.19	0.94	257.18	2.57	1.8	1.2	15.1	10	28.3
3/1/07	9:40:43	3.29	0.93	282.88	3.31	2.4	1.8	20.1	15.1	44.2
3/1/07	9:40:43	1.3	0.95	289.54	3.71	5.0	2.2	42.7	18.8	50.7
3/1/07	9:40:43	−12.94	1	297.44	4.2	1.8	1.2	15.1	10	58.8
3/1/07	9:40:43	−3.26	0.99	298.22	4.47	8.1	1.9	69	16.3	59.2
3/1/07	9:40:51	27.64	2.45	190.1	10.46	29.6	17.8	62.8	37.7	72.6
3/1/07	9:40:51	−26.05	2.19	209.02	6.03	177.6	17.8	376.6	37.7	87.3
3/1/07	9:40:51	−49.92	2.96	216.52	7.28	65.1	23.8	138.1	50.2	91.9
3/1/07	9:40:51	−11.65	1.93	234	5.28	230.0	11.8	489.5	25.1	112
3/1/07	9:40:59	25.97	2.39	191.05	9.97	35.6	11.8	75.3	25.1	73.1
3/1/07	9:40:59	−28.8	2.24	207.95	6.15	183.6	17.8	389.1	37.7	86.3
3/1/07	9:40:59	−52.98	3.15	215.04	7.59	65.1	23.8	138.1	50.2	90.8
3/1/07	9:40:59	16.91	2.07	215.97	6.15	35.6	17.8	75.3	37.7	95.4
3/1/07	9:40:59	−14.17	1.95	234	5.33	230.0	11.8	489.5	25.1	111.7
3/1/07	9:41:07	−26.15	2.2	206.77	6.13	76.9	71.1	163.2	150.6	85.3
3/1/07	9:41:07	−11.04	1.93	232.58	5.28	130.3	59.2	276.1	125.5	110.7
3/2/07	23:50:01	61.62	0.78	123.81	0.78	116,893	27,557	85,000	20,000	69.6
3/2/07	23:50:21	61.29	0.77	124.62	0.8	68901.5	13,780	50,000	10,000	69.1
3/2/07	23:50:24	61.08	0.76	125.17	0.82	67773.2	12,877	49,333	9333.3	68.7
3/3/07	6:11:01	21.42	0.64	230.74	1.38	843.4	84.3	500	50	20

refine the assumed temperature to use in further calculations of brightness.

With one exception, all the MVIC sources appeared only in the methane (CH₄) and near infrared (NIR) filters. The exception, Tvashtar, which was by far the brightest spot, was observed in those filters and the red filter. The methane and near infrared filters are too close in wavelength range to yield meaningful color temperatures. For the single Tvashtar observation in the red filter, we were able to calculate color temperatures based on the measured red/NIR and red/CH₄ ratios. Results are discussed below.

To constrain the temperatures of other hot spots, we investigated the usefulness of combining LORRI and MVIC NIR or CH₄ filter observations. We calculated the filter response in DN for LORRI, MVIC NIR, and MVIC CH₄ for various blackbody temperatures and hotspot areas. We accounted for the range to the target and exposure time in the available data and compared the calculated DN to the measured DN to determine which blackbody temperatures and hotspot areas matched the observations within the uncertainties. We found that a broad range of temperatures and areas fit the data and thus, are unable to significantly constrain these quantities. Furthermore, because of the much stronger dependence of brightness on temperature than on area, the hotspot areas are almost completely unconstrained.

2.3. Determining locations

All of the MVIC images (e.g., Fig. 3) and many of the LORRI images were obtained with part of Io's disk illuminated by sunlight, with hotspots visible on the unilluminated portion of the disk. Due to short exposure times, only the brightest hotspots can be observed in these images. The presence of Io's illuminated limb allows us to determine the location of these hotspots precisely by fitting the limb, particularly in the LORRI data, which are higher resolution than the MVIC images. We use the SPICE system (Acton, 1996) from NASA's Navigation and Ancillary Information Facility (NAIF) to determine the orientation and limb shape of Io at the time of each of the LORRI observations, assuming a triaxial ellipsoid shape for Io. We fit this outline of Io to the limb observed in the images. For each hotspot, we found the centroid of the brightness and computed its location on Io in latitude and

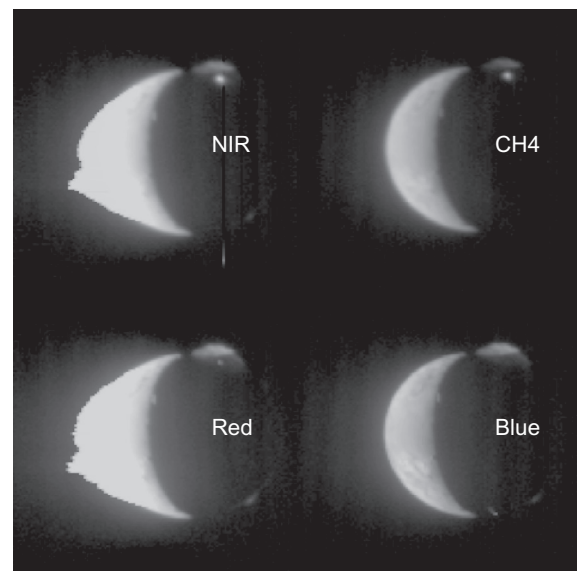


Fig. 3. Logarithmic stretch of an MVIC observation of Io showing the Tvashtar hotspot and plume in the upper right of each image. The sunlit part of Io is overexposed in the NIR and Red filters, leading to bleeding to the left in these images.

longitude, obtaining accuracies of 20 km or better in most cases, based on the resolution of the images.

Once we determined the location of the bright spots measurable in the partially-illuminated images, we used those to refine the locations of other hotspots observed in the eclipse images. The uncertainty in location is larger for the eclipse images than for the partial daytime images due to the accumulating uncertainty of the original hotspot fits with the uncertainty of the measured hotspot. Two eclipses were observed by LORRI, on February 27th and March 1st 2007. We combined the best observations from each eclipse to significantly increase the signal to noise and identify more sites of emission (Fig. 4). Because these fainter spots are only

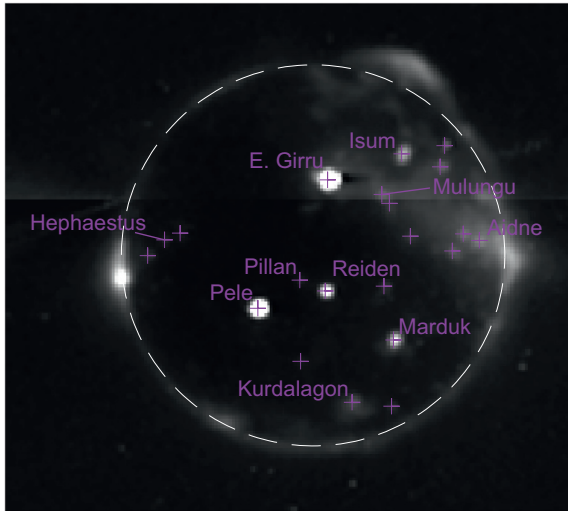


Fig. 4. Total image from averaging most of the 4×4 binned images from the March 1st eclipse, avoiding images contaminated by scattered light from Jupiter. North is approximately up and the central longitude is 240W. Dashed line indicates the SPICE-derived position of the limb registered to the position of E. Girru. Pink plus signs indicate emission sources. Note that all emission sources appear to be point sources at this resolution with the obvious exception of Kurdalagon in the lower right. (For interpretation of the references to color in this figure legend, the reader is referred to the web version of this article.)

measurable with sufficient signal-to-noise in the summed image, we could not observe their temporal variability.

3. Temporal variations

During the February 27th eclipse, 23 LORRI images were obtained at irregular intervals over an hour and a half (Table 2, Fig. 5). Three volcanoes were observed in these images: Reiden, Pele, and E. Girru. While E. Girru showed a slight increase (10–20%), neither Pele or Reiden demonstrated substantial variations during that time, after correcting for changes in emission angle.

During the March 1st eclipse, two sets of images were obtained (Table 2). The same three bright hotspots (E. Girru, Pele, and Reiden) were observed in these images as in the previous eclipse. One set was binned on-chip by 4 by 4 pixels to increase signal to noise at the expense of spatial resolution. Five additional sources were detected in these observations: Kurdalagon, Isum, Marduk, Mulungu, and an unnamed hotspot observed by Galileo at 28N, 192W. The Kurdalagon emission feature differed from the others in that it was measurably extended as opposed to a point source (Fig. 4). Furthermore, when we calculated the equivalent area of a 1200 K blackbody necessary to produce the measured emission, it should have been observed by MVIC, but no such emission was detected by MVIC. We therefore deduce that the flux observed at Kurdalagon was not due to thermal emission and was likely gas emission caused by the interaction of the gas with Io’s magnetosphere. A particulate plume was observed at Kurdalagon in sunlit images and similar diffuse glows were seen at the plumes over N. Lerna (Fig. 7) and Tvashtar (Fig. 4, analyzed by Roth et al., 2011).

Of the seven sources we interpret as volcanic hotspots observed during eclipse at short time-scales, none exhibited measurable variations over tens of seconds (Fig. 5). The New Horizons observations were the first time individual Ionian volcanoes have been observed on such short time scales and demonstrates that the volcanoes have stable brightnesses on these timescales. Radebaugh et al. (2004), using data from Galileo, found no detectable variations in brightness on a timescale of several minutes, and that all

Table 2
Summary of LORRI data obtained during each eclipse.

Date	Start time	End time	# Images	Notes
2/27/2007	14:30	16:00	23	
3/1/2007	9:30	9:31	39	Binned on chip 4×4
3/1/2007	9:35	9:40	27	

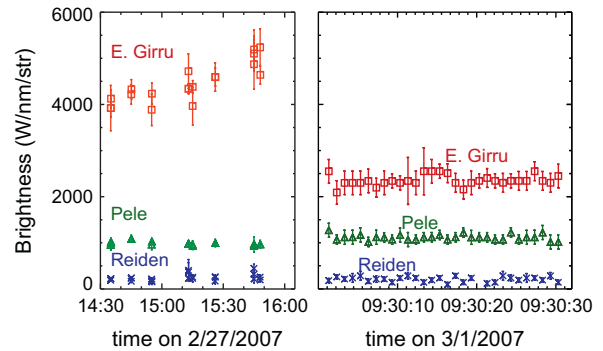


Fig. 5. Brightness at 757 nm of three volcanoes during the two eclipses, from LORRI images. Note the difference in time-scales and the time gap between the two eclipses.

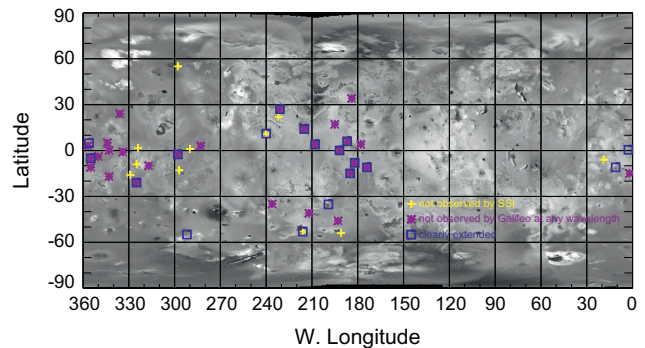


Fig. 6. Location of emission sources identified by LORRI that were not found by SSI, overlaid on an SSI global basemap. Sources that are clearly extended in nature (not point sources in the images) are also noted.

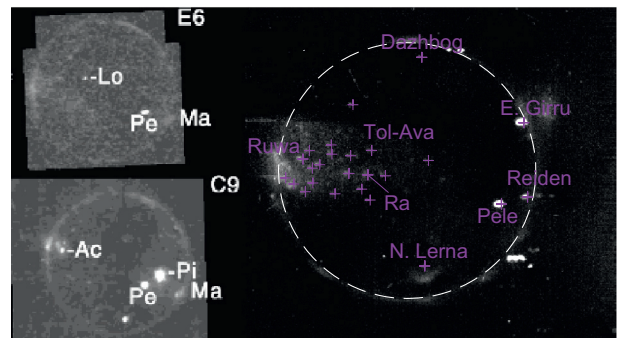


Fig. 7. At Right: Labeled co-added LORRI image from the February 27 eclipse. North is approximately up and the central longitude is 305W. Left: Two eclipse images from Galileo SSI (from McEwen et al., 1998b). All show a background glow near the limb of Io. Bright spots beyond Io’s limb are background stars and diffuse emission is internal reflection in the camera.

changes were due to emission angle effects. Our results confirm that changes in Ionian volcanoes, if they occur, generally occur over timescales of hours or longer. This indicates that the thermal emission for these hot spots at this time is dominated by an

emplacement process that does not vary greatly on short time-scales, which favors lava flows as opposed to more energetic phenomena like lava fountains (Keszthelyi et al., 2007). Of the 4 volcanoes observed over the timescale of days (Tvashtar, Pele, E. Girru, and Reiden), only E. Girru shows detectable changes over the several days of observations (see discussion in next section).

4. Changes from Galileo to New Horizons

The Galileo Solid State Imager (SSI) obtained eclipse images in an open filter with a nearly identical wavelength range to LORRI, enabling comparisons on a decade time scale by comparing images obtained by Galileo from 1996 to 2001 to the New Horizons observations from 2007. SSI observed 44 emission sources over 14 eclipses covering the entire globe (Lopes et al., 2007). Brightnesses of these sources in physical units have not been published, although temperature and area fits were published for the observations obtained during early orbits (McEwen et al., 1998b). Of the 44 sources, Pele was observed most often by Galileo SSI, followed by Pillan, Kanehekili, Amarani, Acala, Loki, Marduk, Ruwa, and Zal. We consider these 9 hot spots to be persistent high-temperature sources. All except Ruwa were also observed by the Galileo Near-Infrared Mapping Spectrometer (NIMS) as having emission at near-infrared wavelengths (Lopes et al., 2007) and the lack of detection of Ruwa by NIMS was likely an effect of poor spatial resolution at this location.

We located a total of 54 emission sources in the LORRI images which covered only 60% of the surface (missing longitudes 30–170W) (Table 1). Thus, LORRI detected twice as many emission sources as SSI per fraction of the disk observed. Of the 9 persistent Galileo high-temperature sources, Kanehekili, Amirani and Zal are located in the longitude range not covered by New Horizons. Of the remainder, Pele and Marduk were observed by New Horizons in multiple images and Pillan and Ruwa were fainter and observed only in co-added eclipse images (Figs. 4 and 8). Acala and Loki were not detected, which may indicate that high-temperature volcanism has ceased at these locations. Dazhbog and Llew were observed by LORRI but not Galileo SSI, but were confirmed as hotspots from other Galileo instruments. The absence in SSI and presence in LORRI indicates that something has changed (perhaps a new high-temperature eruption) at these locations (Lopes et al., 2007).

Of the 54 emission sources observed by New Horizons, 40 had not been previously observed by SSI, 31 had not been previously observed by any instrument, and 13 were clearly extended sources

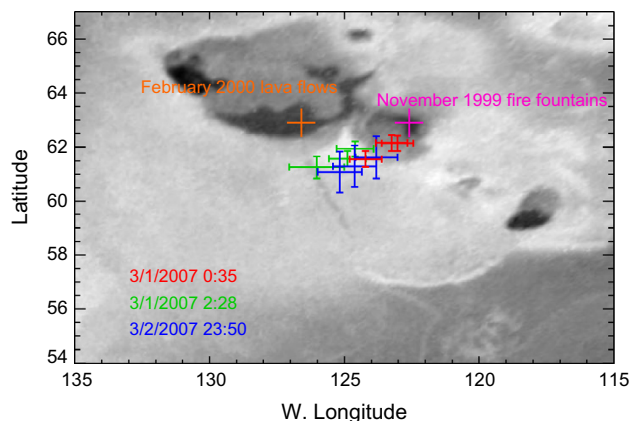


Fig. 8. Location of Tvashtar eruption locations overlaid on the SSI basemap. Orange and pink show the locations of Galileo era eruptions (Lopes et al., 2007) while the red, green, and blue show the locations measured by New Horizons over 2 days. (For interpretation of the references to colour in this figure legend, the reader is referred to the web version of this article.)

(Fig. 6). McEwen et al. (1998b) analyzed SSI observations of active volcanism on Io during the first 10 orbits of the Galileo spacecraft. Those data included 25 images obtained of Io in eclipse. They identified 32 hot spots (thermal emission) in those images plus a field of ~ 26 bright spots near the sub-Jupiter point. Many of the New Horizons sources are similarly located in regions that appear bright in eclipse and are located near the Jupiter-facing and anti-Jupiter points (Fig. 7). We also found that most of these are near identified paterae, but not necessarily dark paterae, which have been interpreted to be active (McEwen et al., 1985). Geissler et al. (2004) found similar small discrete sources in low-resolution Cassini visible light eclipse images. They found that the equatorial glows are also bright in the near-ultraviolet indicating non-thermal (atmospheric) emission. Because of the concentration of the discrete emission sources in regions of enhanced atmospheric emission, the fact that many are extended, and do not correlate with thermal emission seen by LEISA (Spencer et al., 2007), we agree with Spencer et al. (2007) that many of these faint sources are probably non-thermal in origin and likely due to gas emission caused by the interaction of the gas with Io's magnetosphere. However, these spots do not correspond to plumes seen in sunlight, so the exact mechanism may be different from the cause of the diffuse glows at Kurdalagon, N. Lerna, and Tvashtar.

5. Individual volcanoes

5.1. Tvashtar

A major eruption at Tvashtar was observed by the Galileo spacecraft (Milazzo et al., 2005) in November 1999, and it included active fire fountains and lava flows. Galileo NIMS measured a color temperature of 1060 ± 60 K (Lopes et al., 2001) while SSI inferred a temperature of 1300–1400 K (Milazzo et al., 2005). The fire fountains were located in the middle patera of the chain of paterae at Tvashtar and had an area of 25 km^2 (Fig. 8). In February 2000, thermal emission from an active lava flow was observed in the western patera. SSI measured a color temperature of 1300 K over 6.3 km^2 and a brightness temperature of 1220–1240 K over an area of 0.1 km^2 from parts of this active flow (Milazzo et al., 2005). New Horizons detected a particulate plume at Tvashtar in 2007 and determined a temperature from LEISA spectra of 1287 K (Spencer et al., 2007).

Tvashtar was by far the brightest hotspot observed by New Horizons. It was observed 3 times by LORRI always on the night side of partially sunlit images. In these images, obtained over 2 days, the emission angle varied between 68° and 78° . The variation in power output with emission angle matches a cosine dependence (Fig. 9), indicating that the emission was from horizontal surfaces such as surface flows as opposed to fire fountains, which would be expected to vary less with emission angle due to their vertical extent (or, less likely, that temporal variability over the two days coincidentally mimicked a cosine variation with emission angle). The location of the emission is closer to the location of the eruption observed by the Galileo spacecraft in November 1999 than that from February 2000 (Fig. 8). Although we were unable to determine a blackbody fit to all the data simultaneously, we determined the color temperature of Tvashtar based on the ratio of observed MVIC brightnesses in different filters. These observations were nearly simultaneous and yielded temperatures of 1240 ± 60 K for the Red/NIR ratio and 1280 ± 100 K for the red/ CH_4 ratio. Using 1280 K as the temperature, a flow size of 30 km^2 best matches the absolute fluxes, while using 1240 K yields a flow size of 50 km^2 best matches. Both sizes are larger than the 25 km^2 determined for the 1999 fire fountains.

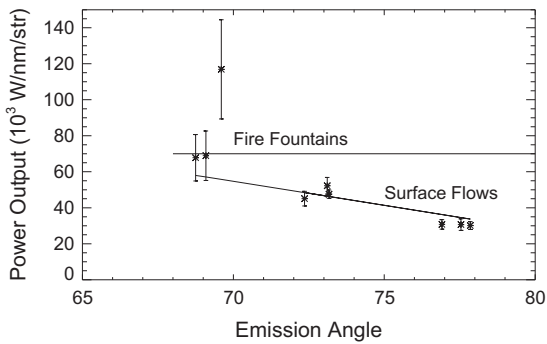


Fig. 9. Measured brightnesses of the Tvashtar hotspot at 757 nm as a function of emission angle. The variation matches that expected from a surface flow, rather than being constant with emission angle as might be expected from a structure with large vertical extent such as a fire fountain. These brightnesses are from the same observations shown in Fig. 8.

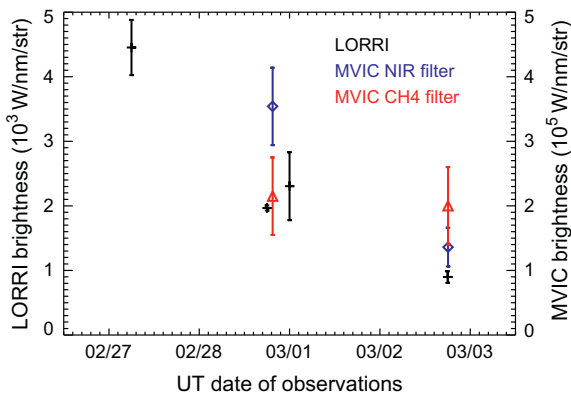


Fig. 10. Brightness of the E. Girru hotspot as a function of time as measured by New Horizons LORRI (757 nm, in black), the MVIC NIR filter (876 nm, in blue), and the MVIC CH₄ filter (888 nm, in red). Measurements have been corrected for emission angle. (For interpretation of the references to colour in this figure legend, the reader is referred to the web version of this article.)

5.2. “East Girru”

East Girru was not previously observed as a thermal source from Voyager, Galileo, or from the ground. It was the second brightest source observed by New Horizons and was detected by both LORRI and MVIC, though MVIC detected E. Girru only in the overlapping near infrared and methane filters, preventing determination of a color temperature. Over the course of the 6 days of

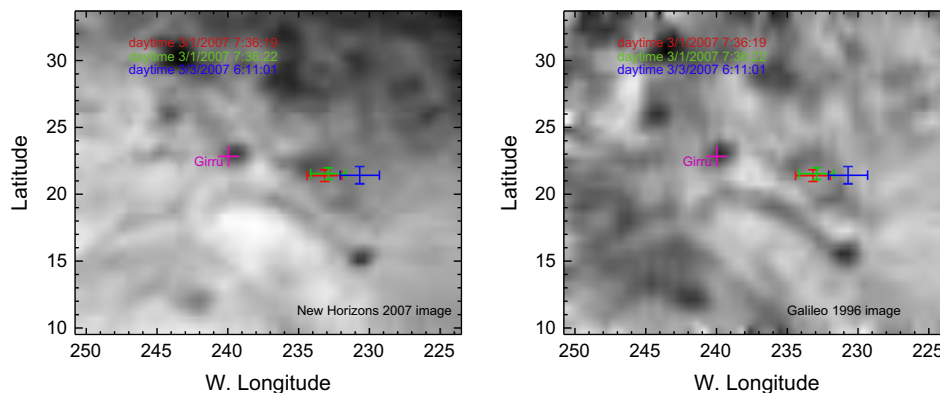


Fig. 11. Left: Highest resolution (15 km/pixel) LORRI image of E. Girru region with location of observed hotspots superimposed. The location of Girru is shown for comparison. Right: Galileo SSI basemap with resolution degraded to match the LORRI image. No significant differences can be detected at the site of the new eruption. The location also lacks a clearly defined region of very low albedo of the type frequently associated with new eruptions, comparable to the dark feature observed at Girru.

LORRI data, a decrease in brightness of more than a factor of 4 was detected after correcting for emission angle (Fig. 10). Smaller decreases were detected in two MVIC filters (near infrared and methane) over 3 days.

The location of E. Girru was well determined using LORRI images that included part of Io’s disk in sunlight. The emission is located approximately 200 km to the east of the previously detected Girru hotspot seen by Galileo. Galileo images show no obvious very low albedo region near this new emission region and New Horizons images, while lower spatial resolution, show no surface changes (Fig. 11). The highest LORRI resolution obtained was on February 27 at 15 km/pixel. Reducing the resolution of the USGS Galileo black and white mosaic to the same resolution shows that no changes occurred in this region (Fig. 11). Nearly all thermal emission regions on Io are correlated with a low albedo feature (e.g. McEwen et al., 1998b), yet there is no conspicuous dark feature at East Girru in the LORRI images. The eruption source could be very small, below the spatial resolution of the best image or the eruption could be very recent, perhaps just beginning in February 2007 (which would be consistent with the rapid flux changes seen by New Horizons (Figs. 5 and 10). However, new eruptions are often accompanied by plumes and no dust plume was observed in reflected sunlight by NH at this location (Spencer et al., 2007). An unusual detached region of diffuse auroral emission was seen above E. Girru in LORRI eclipse (Fig. 7) and Hubble Space Telescope Far Ultra-Violet images (Retherford et al., 2007; Spencer et al., 2007; Roth et al., 2011), suggesting that there may have been some gas output from this source.

5.3. Pele

Pele is one of the most persistent sources of thermal emission on Io, especially in the shorter wavelengths: its thermal emission was first seen by Voyager in 1979. A very high-spatial resolution (~200 m/pixel) Galileo nighttime observation of Pele’s thermal emission is shown in red/yellow pseudocolor in Fig. 13. The color temperature in each pixel ranges from 1270 K to 1605 K (Radebaugh et al., 2004). Cassini obtained observations of Pele’s thermal emission on the timescale of minutes and found that the total intensity varied little on that time scale (after correcting for emission angle) similar to our LORRI observations (Radebaugh et al., 2004). Since only LORRI observed Pele, we were unable to determine its temperature from New Horizons data.

Pele was observed by LORRI during both eclipses. During the March 1 eclipse, the spatial resolution was high enough, 15 km/pixel at Pele’s location, to reveal Pele as a double hotspot (Fig. 12). The two thermal emissions regions were of roughly equal

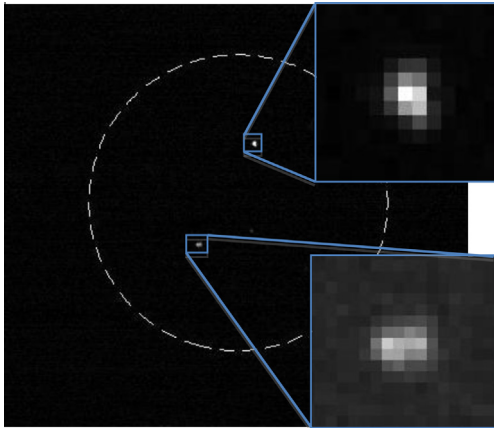


Fig. 12. Mean of images from the March eclipse. The dotted line indicates the position of Io's limb. The brightest spot is E. Girru. The double spot in the lower left is Pele. The Pele spot is clearly more extended than the E. Girru point source and consists of two bright areas surrounded by less bright pixels.

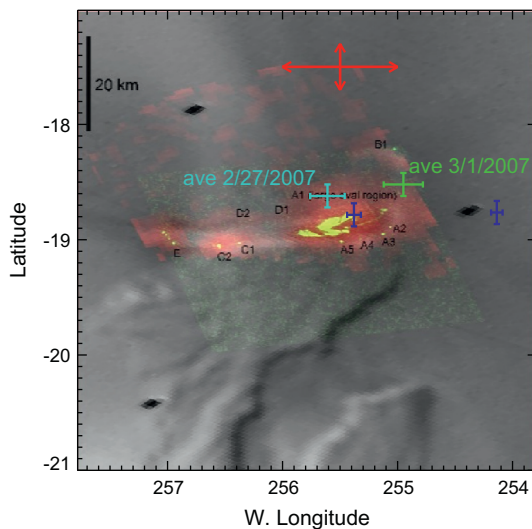


Fig. 13. Position of Pele hotspot determined from LORRI images overlaid on Galileo data (from Howell and Lopes, 2011). The background image is Voyager clear filter, the red component is NIMS emission at $1.03 \mu\text{m}$, and the green (which shows as yellow because it is mostly superposed on the above red) is nighttime SSI at $0.968 \mu\text{m}$. The dated locations in green and teal are from co-added, and therefore lower-resolution, New Horizons eclipse images and are average locations while the lower two locations in blue are from the double hotspot observation shown in Fig. 9. While we are confident of the relative positions of the blue, green, and teal points, their absolute position relative to the Galileo images is uncertain by an amount indicated by the red arrows. (For interpretation of the references to colour in this figure legend, the reader is referred to the web version of this article.)

brightness and separated by about 40 km (Fig. 13). High spatial resolution Galileo SSI images ($\sim 60 \text{ m/pixel}$) revealed a complicated pattern of thermal emission, with multiple sources over approximately 60 km (Howell and Lopes, 2011). Observations by SSI and NIMS showed that while the pattern changed on the time-scale of months, there was always a single dominant bright area. The New Horizons observation therefore shows a different configuration of emission from Pele than was ever seen by Galileo, though with a similar overall extent. Howell and Lopes (2011) used the New Horizons LEISA observations over $1.5\text{--}2.5 \mu\text{m}$, which are well fit by a 1300 K blackbody (Spencer et al., 2007), to estimate the expected $1.03 \mu\text{m}$ New Horizons era brightness. They found that this brightness is roughly a factor of five less than the $1.03 \mu\text{m}$

signal measured during the Galileo I32 flyby in 2001. Accounting for that decrease in the main Pele spot they observed, an increase by a factor of 6 would still be required in the fainter spot in order to have the two spots of equal brightness as we observe with LORRI.

6. Conclusions

We located 54 total emission sources in the New Horizons LORRI and MVIC data and determined their brightnesses. Tvashtar and E. Girru were observed by both LORRI and MVIC, both in the NIR and CH_4 filters. Tvashtar was additionally observed in the red filter, which allowed us to calculate a color temperature of approximately 1260 K .

We used these data to address several questions regarding the state of Ionian volcanism. We found that thirteen of the volcanoes that exhibited high-temperature emission during the Galileo era (observations ended in 2001) continued to do so in 2007. There have been some changes to the short-wavelength output (indicative of high temperatures) of at least 4 volcanoes, with Acala and Loki showing no detectable emission in 2007 and Dazhbog and Llew showing none during Galileo.

The observations allowed us to look for changes in emission on timescales that have been poorly explored in the past. At the short end, which Galileo was unable to explore, none of the seven volcanoes observed showed substantial changes on the order of seconds. Furthermore, only E. Girru exhibited substantial variation over minutes to days.

We determined that the locations of the brightest emission from Tvashtar and Pele had moved slightly between Galileo and New Horizons. The new E. Girru hotspot is located approximately 200 km east of the Galileo-era Girru hotspot. Given the lack of evidence for such long lava flows on Io forming over such a short period of time (Keszthelyi et al., 2001; Williams et al., 2007), we interpret E. Girru to be a new volcanic eruption. Its emission increased by 10% over several minutes during one eclipse, indicating current vigorous activity, though there was an overall decline during the New Horizons flyby. The highest resolution LORRI and Galileo images of this region indicate no noticeable changes and no obvious very low albedo region as is normally observed at active volcanic sites (McEwen et al., 1985). This is one of the major puzzles presented by the New Horizons data: What is the surface source of the high temperature emission from E. Girru? A possibility is that this eruption was a fissure eruption in its early stages, possibly similar to that of Thor observed in 2001 by Galileo, in which thermal output was enough to cause saturation at NIMS wavelengths (Lopes et al., 2004) but when the SSI camera imaged the region about two months later, thin lava flows were seen, which would not have been detectable at the resolution of New Horizons. However, in the case of Thor, a tall plume was detected (Turtle et al., 2004).

Observations of Tvashtar are consistent with a current eruption similar to previously observed eruptions, though less energetic than the November 1999 Galileo observations in that observations are more consistent with a lava flow than the fire fountains inferred from the November 1999 observations (Milazzo et al., 2005). The measured temperature, location, and size are similar to previously observed eruptions at this site, although the location changed.

Pele's eruption appears to have changed. During the Galileo era, it consistently exhibited a single major thermal source with multiple smaller sources and subtle changes in the emission pattern. New Horizons observed two sources of roughly equivalent emission, indicating a change in eruption style.

New Horizons LORRI identified twice as many emission sources per fraction of the disk observed than Galileo SSI did. Many of them

are very likely indicative of high-temperature volcanism, especially at locations also observed by MVIC or previously observed in the near infrared. However, many of the sources are either extended, do not correlate with previously identified volcanism, or were located in large bright regions that appear to be related to interactions between the magnetosphere and atmosphere. Most of these are likely due to non-thermal activity. Extended glows at Kurdalagon, N. Lerna, and Tvashtar (Roth et al., 2011) correspond to plumes seen in sunlight, while the smaller glows do not. The exact process that creates these glows is another of the major questions posed by the analysis of the New Horizons data.

Acknowledgments

We would like to thank Lucas Kamp, who assisted with data reduction, Eric Bloss and Kyle McMillian, who assisted as summer undergraduate researchers, and two anonymous reviewers. Part of this work was carried out at the Jet Propulsion Laboratory, California Institute of Technology, under contract with NASA. This project was supported by the NASA Jupiter Data Analysis Program and the JPL summer faculty Fellowship program.

References

- Acton, C.H., 1996. Ancillary data services of NASA's navigation and ancillary information facility. *Planet. Space Sci.* 44, 65–70.
- Cheng, A.F. et al., 2008. Long-range reconnaissance imager on New Horizons. *Space Sci. Rev.* 140, 189–215.
- Davies, A.G. et al., 2001. Thermal signature, eruption style, and eruption evolution at Pele and Pillan on Io. *J. Geophys. Res.* 106, 33079–33104.
- Davies, A.G., Veeder, G.J., Matson, D., Johnson, T.V., 2012. Charting thermal emission variability at Pele, Janus Patera and Kanehekili Fluctus with the Galileo NIMS Io Thermal Emission Database (NITED). *Icarus* 221, 466–470.
- Geissler, P., McEwen, A., Porco, C., Strobel, D., Saur, J., Ajello, J., West, R., 2004. Cassini observations of Io's visible aurorae. *Icarus* 172, 127–140.
- Howell, R.R., Lopes, R.M.C., 2011. Morphology, temperature, and eruption dynamics at Pele. *Icarus* 213, 593–607.
- Keszthelyi, L. et al., 2001. Imaging of volcanic activity on Jupiter's moon Io by Galileo during the Galileo Europa Mission and the Galileo Millennium Mission. *J. Geophys. Res.* 106, 33025–33052.
- Keszthelyi, L., Jaeger, W., Milazzo, M., Radebaugh, J., Davies, A.G., Mitchell, K.L., 2007. New estimates for Io eruption temperatures: Implications for the interior. *Icarus* 192, 491–502.
- Lopes, Rosaly M.C. et al., 2001. Io in the near infrared: Near-Infrared Mapping Spectrometer (NIMS) results from the Galileo flybys in 1999 and 2000. *J. Geophys. Res.* 106, 33053–33078.
- Lopes, R., Kamp, L.W., Smythe, W.D., Mouginiis-Mark, P., Kargel, J., Radebaugh, J., Turtle, E.P., Perry, J., Williams, D.A., Carlson, R.W., Douté, S., 2004. Lava Lakes on Io. Observations of Io's volcanic activity from Galileo during the 2001 fly-bys. *Icarus* 169, 140–174.
- Lopes, R.M.C., Radebaugh, J., Meiner, M., Perry, J., Marchis, F., 2007. Appendix 1 in Io after Galileo: A new view of Jupiter's Volcanic Moon. In: Lopes, R.M.C., Spencer, J.R. (Eds.), pp. 307–323.
- McEwen, A.S., Soderblom, L.A., Matson, D.L., Johnson, T.V., 1985. Volcanic hot spots on Io – Correlation with low-albedo calderas. *J. Geophys. Res.* 90, 12345–12379.
- McEwen, A.S. et al., 1998a. High-temperature silicate volcanism on Jupiter's moon Io. *Science* 281, 87–90.
- McEwen, A.S., Keszthelyi, L., Geissler, P., Simonelli, D.P., Carr, M.H., Johnson, T.V., Klaasen, K.P., Breneman, H.H., Jones, T.J., Kaufman, J.M., Magee, K.P., Senske, D.A., Belton, M.J.S., Schubert, G., 1998b. Active volcanism on Io as seen by Galileo SSI. *Icarus* 135, 181–219.
- Milazzo, M.P., Keszthelyi, L.P., Radebaugh, J., Davies, A.G., Turtle, E.P., Geissler, P., Klaasen, K.P., Rathbun, J.A., McEwen, A.S., 2005. Volcanic activity at Tvashtar Catena, Io. *Icarus* 179, 235–251.
- Morgan, F. et al., 2005. Calibration of the New Horizons long-range reconnaissance imager. *Proc. SPIE* 5906, 421–432.
- Radebaugh, J., McEwen, A.S., Milazzo, M.P., Keszthelyi, L.P., Davies, A.G., Turtle, E.P., Dawson, D.D., 2004. Observations and temperature of Io's Pele Patera from Cassini and Galileo spacecraft images. *Icarus* 169, 65–79.
- Rathbun, J.A., Spencer, J.R., 2010. Ground-based observations of time variability in multiple active volcanoes on Io. *Icarus* 209, 625–630.
- Rathbun, J.A., Spencer, J.R., Davies, A.G., Howell, R., Wilson, L., 2002. Loki Io: A periodic volcano. *Geophys. Res. Lett.* 29, 84–1–84–4.
- Reuter, D.C. et al., 2008. Ralph: A visible/infrared imager for the New Horizons Pluto/Kuiper Belt Mission. *Space Sci. Rev.* 140, 129–154.
- Retherford, K.D., Spencer, J.R., Stern, S.A., Saur, J., Strobel, D.F., Steffl, A.J., Gladstone, G.R., Weaver, H.A., Cheng, A.F., Parker, J.W., Slater, D.C., Bersteeg, M.H., Davis, M.W., Bagenal, F., Throop, H.B., Lopes, R.M.C., Reuter, D.C., Lunsford, A., Conard, S.J., Young, L.A., Moore, J.M., 2007. Io's Atmospheric response to eclipse: UV aurorae observations. *Science* 318, 237–240.
- Roth, L., Saur, J., Retherford, K.D., Strobel, D.F., Spencer, J.R., 2011. Simulation of Io's auroral emission: Constraints on the atmosphere in eclipse. *Icarus* 214, 495–509.
- Spencer, J.R. et al., 2007. Io volcanism seen by New Horizons: A major eruption of the Tvashtar volcano. *Science* 318, 240–243.
- Tokunaga, A.T., Vacca, W.D., 2005. The mauna kea observatories near-infrared filter set. III. Isophotal wavelengths and absolute calibration. *Publ. Astron. Soc. Pac.* 117, 421–426.
- Turtle, E.P., Keszthelyi, L.P., McEwen, A.S., Radebaugh, J., Milazzo, M., Simonelli, D.P., Geissler, P., Williams, D.A., Perry, J., Jaeger, W., Klaasen, K.P., Breneman, H.H., Denk, T., Phillips, C.B. the Galileo SSI Team, 2004. The final Galileo SSI observations of Io: orbits G28–I33. *Icarus* 169, 3–28.
- Williams, D.A., Keszthelyi, L.P., Crown, D.A., Jaeger, W.L., Schenk, P.M., 2007. Geologic mapping of the Amirani-Gish Bar region of Io: Implications for the global geologic mapping of Io. *Icarus* 186, 204–217.